Food Chemistry: X 23 (2024) 101722

Contents lists available at ScienceDirect

Food Chemistry: X

journal homepage: www.sciencedirect.com/journal/food-chemistry-x

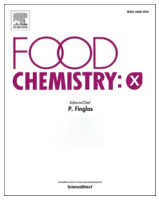

Revealing salt concentration for microbial balance and metabolite enrichment in secondary fortified fermented soy sauce: A multi-omics perspective

Lin Zhang, Zhu Zhang, Jun Huang, Rongqing Zhou *, Chongde Wu

College of Biomass Science and Engineering, Sichuan University, Chengdu, 610065, China

A R T I C L E I N F O

Chemical compounds studied in this article:
Lactic acid (PubChem CID: 612)
Succinic acid (PubChem CID: 1110)
Glutamic acid (PubChem CID: 33032)
Histamine (PubChem CID: 774)
4-Ethylguaiacol (PubChem CID: 62465)
2-Ethyl-4-hydroxy-5-methyl-3(2H)-furanone (PubChem CID: 33931)
Met-Gly-Met (PubChem CID: 40496734)

Keywords:
Fortified soy sauce
Salt reduction
Metabolites
Shotgun metagenomics
Metabolome-microbiome interactions

A B S T R A C T

This study examined the impact of varying salt concentrations on microbiota, physicochemical properties, and metabolites in a secondary fortified fermentation process using multi-omics techniques. It aimed to determine the influence of salt stress on microbiota shifts and metabolic activities. The findings demonstrated that moderate salt reduction (MS) was found to enhance moromi's flavor and quality, while mitigating the negative effects of excessive low salt (LS). MS samples had 1.22, 1.13, and 2.92 times more amino acid nitrogen (AAN), non-volatiles, and volatiles, respectively, than high salt (HS) samples. In contrast, lactic acid and biogenic amines in LS samples were 1.56 g/100 g and 4115.11 mg/kg, respectively, decreasing to 0.15 g/100 g and 176.76 mg/kg in MS samples. Additionally, the contents of ethanol and small peptides increased in MS due to the growth of specific functional microorganisms such as *Staphylococcus gallinarum*, *Weissella confusa*, and *Zygosaccharomyces rouxii*, while food-borne pathogens were inhibited. Network analysis revealed that the core microbial interactions were enhanced in MS samples, promoting a balanced fermentation environment. Redundancy analysis (RDA) and correlation analyses underscored that the physicochemical properties significantly impacted bacterial community structure and the correlations between key microbes and flavor compounds. These findings provided a theoretical foundation for developing innovative reduced-salt fermentation techniques, contributing to the sustainable production of high-quality soy sauce.

1. Introduction

Soy sauce, renowned for its distinct flavor, contributed by the synergistic effect of functional microbiota, has gained widespread popularity across various countries and regions globally (Gao, Zhao, et al., 2023). Its production relies on two primary methods: low-salt solid-state fermentation (LSF) and high-salt liquid-state fermentation (HLF), with the latter being more prevalent in China, Japan, and Southeast Asian countries due to its unique flavor profile and nutritional benefits (Feng et al., 2014). The conventional HLF process, typically conducted over 6–12 months, involves koji manufacture, moromi fermentation, *etc* (Gao, Zhao, et al., 2023). The concentration of NaCl in brine is a crucial abiotic factor influencing the development and succession of functional microbiota, modulating interspecific interactions within the microbiota as well as metabolic and nutrition networks (Liu et al., 2023), thereby significantly affecting the quality and flavor of fresh soy sauce. However, this time-intensive method not only results in high salt content (18%–20%) in fresh soy sauce but also risks contamination with endogenous hazards like ethyl carbamate and biogenic amines (BAs), posing biosafety threats (Gao, Li, et al., 2023). Over the past two decades, a method known as secondary fortified fermentation, aimed at producing high-quality soy sauce with better taste and aroma, has garnered attention. This method involves incorporating a portion of mature soy sauce from the preceding fermentation cycle into the raw materials, blending it with fresh brine to achieve an amino acid nitrogen (AAN) content of 0.4–0.6 g/100 mL, and subsequently undergoing refermentation with fresh koji (Jiang, Chen, et al., 2023). Despite these advancements, reducing salt concentration remains challenging due to the health risks of excessive sodium intake, including cardiovascular diseases, and the difficulty of treating waste with high sodium chloride levels (Hu et al., 2023). Reducing salt contents in soy sauce fermentation may compromise its preservative capacity, as demonstrated by failed fermentation and increased presence of pathogens, including *Bacillus*, *Kurthia*, *Staphylococcus saprophyticus*, and *Lactobacillus pobuzihii* when

* Corresponding author.
E-mail address: zhourqing@scu.edu.cn (R. Zhou).

https://doi.org/10.1016/j.fochx.2024.101722
Received 4 July 2024; Received in revised form 5 August 2024; Accepted 7 August 2024
Available online 8 August 2024

NaCl content is reduced to 12% in moromi (Hu et al., 2023). In the context of Chinese soy sauce, excessively low salt levels have resulted in the absence of key flavor compounds such as benzyl alcohol, 5-methylfuraldehyde, phenylacetic acid, guaiacol, and 4-ethylguaiacol (4-EG), thereby adversely affecting the overall flavor profile (Liu et al., 2023). Similarly, research on reduced-salt doubanjiang has indicated higher total acidity and BAs in the presence of conditionally pathogenic bacteria, such as *Klebsiella*, *Cronobacter*, and *Acinetobacter*, despite increased AAN, amino acids, and volatiles (Yang et al., 2021).

To address these issues, various alternative technologies have been explored, including substituting sodium chloride with potassium or calcium salt or using yeast extracts and desalinating the fresh soy sauce (Crowe-White et al., 2023; Kingwascharapong et al., 2024; Wang et al., 2021). However, these methods have inherent limitations, such as introducing off-flavors, disrupting the balance of the profiles of the characteristic aroma and flavor profiles, and the high costs of equipment and operation (Zhang et al., 2020). Strategies involving the use of endogenous or exogenous functional isolates or microbiota for salt reduction have shown promise (Hu et al., 2024). For example, Singracha et al. (2017) demonstrated that the functional isolates and synthetic microbiota in reduced-salt moromi (12% NaCl) fermentation enhanced certain key volatiles, acetic acid, and histamine, decreased maltol and guaiacol, whereas the effects on non-volatiles, excluding organic acids, remained unclear. Hu et al. (2024) found that aroma and saltines were also improved in reduced-salt moromi (12% NaCl) using similar methods. Introducing a bacterial starter to northeastern Chinese sauerkraut with 0.5% salt increased lactic acid bacteria and flavor compounds (Yang et al., 2020). Using yeast starters to reduce salt in table olive fermentation matched the conventional process's microbiota succession (Penland et al., 2022). The secondary fortified fermented process introduces soluble nitrogenous substances, flavor compounds, and coordinated brewing microbiota from the start. However, the impact of the microbial isolates or synthetic microbiota inoculation on microbial community succession and metabolism under varying salt stress during new fermentation processes remains unclear.

In this study, we aimed to investigate the impact of salt concentration on microbiota, physicochemical properties, and metabolites in soy sauce fermentation, utilizing multi-omics techniques. We explore how salt stress affects microbiota in high-salt environments from prior fermentation cycles by correlating microbiomes and metabolites. Our goal is to offer insights that could guide the development of innovative, reduced-salt techniques for liquid-state soy sauce fermentation.

2. Materials and methods

2.1. Chemicals

Organic acids standard, biogenic amines standard, and internal standard (1,7-Diaminoheptane, methyl caprylate, and decanoic acid-d_{19}) were chromatographic grade (Sigma-Aldrich). The free amino acid (FAA) mixture standards were purchased from the instrument supplier (A300, membraPure GmbH, Germany). Physicochemical properties testing reagents for chemical analysis, were sourced locally.

2.2. Moromi fermentation

Finished koji produced by *A. oryzae* 3.042 in 36 h was obtained from Qianhe Condiment Co., Ltd. (Meishan City, Sichuan Province, China) to ensure consistency. The finished koji exhibited a neutral protease activity was 879 U/g and a moisture content of 30%. A brine was prepared by adjusting the AAN content to 0.6 g/100 mL using raw soy sauce, containing varying concentrations of NaCl, at a ratio of 1:1.8, resulting in moromi with a salt content of 16% (HS), 13% (MS), and 10% (LS) (*w*/w). Placed in 5 L glass bottles, they were covered with gauze and incubated at 30 °C for 90 days. Three biological replicates were prepared for each variant. The moromi was stirred every 2nd day for the first 15 days, then every 5th day. Sampling was carried out every five days for the first month, then every ten days until the fermentation ended. Each sample was mixed well before taking 500 g; half was stored at −20 °C for physiochemical and metabolite analysis (for a maximum of a week), while the other half was stored at −80 °C for microbial community structure analysis (for a maximum of two weeks).

2.3. Detection of physicochemical properties

Analyses of total acidity (TA), ammonia nitrogen (AN), reducing sugar (RS), amino acid nitrogen (AAN), total nitrogen (TN), and NaCl were measured using titration, the methodology described by Zhang et al. (2024). Ethanol content was determined using the potassium dichromate method (Zhang et al., 2021).

2.4. Detection of organic acids, biogenic amines, and free amino acids

The contents of organic acids (OAs), BAs, and FAAs were analyzed according to the methods described by Zhang et al. (2024). Briefly, samples were extracted with 9 mM H_2SO_4, sonicated, filtered through a C18 SPE column (Swell Scientific Instruments Co., Ltd., Chengdu, China) and a 0.22 μm membrane filter (Micron Separation Inc., Westborough, MA), then injected into an Agilent 1260 HPLC system (Agilent Technologies, Santa Clara, CA, USA). The system equipped with an Avantor Hichrom OA-1000 organic acid column (300 × 6.5 mm; VWR International, Lansdale, PA, USA), used a 9 mM H_2SO_4 mobile phase at 0.60 mL/min, with detection at 215 nm.

For BAs, samples were extracted with 0.4 M perchloric acid, then centrifuged post-mixing. 1 mL supernatant was treated with 0.2 mL of 2 M NaOH, 0.3 mL of saturated $NaHCO_3$, and 2.0 mL of dansyl chloride solution (10 mg/mL, acetone) in a brown vial, stirred in the dark at 40 °C for 45 min, then quenched with 0.1 mL of 25% ammonia. The extract was diluted to 5 mL with acetonitrile and filtered. The gradient elution utilized two solvents: eluent A, consisting of 90% acetonitrile and 10% ammonium acetate solution (0.01 mol/L with 1% acetic acid), and eluent B, composed of 10% acetonitrile and 90% ammonium acetate solution (0.01 mol/L with 1% acetic acid). The gradient started at 60% A, increased to 85% A at 22 min, reached 100% A at 32 min, and returned to 60% A at 32.01 min, held until 37 min, with a flow rate of 0.8 mL/min. Analysis was performed on an Agilent 1260 HPLC with a UV detector at 254 nm, using an SVEA GOLD C18 column (5 μm, 4.6 × 250 mm; Nanologica, Sodertalje, Sweden) at 35 °C, with 20 μL injections.

For FAAs, samples were extracted and purified by HCl (0.01 mol/L) and 20% sulfosalicylic acid solution for at least 1 h, respectively, and then determined by Amino acid analyzer (A300, membraPure GmbH, Germany) after being filtered through 0.22 μm filter. The quantification of FAAs was performed using the external standard method with 100 nmol/mL L-amino acids under the same chromatographic conditions.

2.5. Detection of non-targeted metabolomics analysis

Post-fermentation, the three moromi samples were assessed for non-volatile compounds using the method described by Chang et al. (2024), with minor modifications, and each sample was analyzed six times. Briefly, 25 mg moromi was extracted with a 500 μL methanol: acetonitrile: water (2:2:1, *V*/V) solution, containing 0.03 μg/mL decanoic acid-d_{19} as an internal standard. The mixture was vortexed for 30 s, homogenized at 35 Hz for 4 min, and then sonicated using an ultrasonic cleaner (PS-60AL, Shenzhen Leaderbang Electronic Co., Ltd.) at a frequency of 40 kHz and a power of 480 watts for 5 min in a water bath at a temperature of 4 ± 1 °C, with the process repeated three times per sample. The resulting supernatants were incubated at 40 ± 1 °C for 1 h, and after centrifugation at 12,000 *g* for 15 min at 4 °C, were analyzed using LC-MS/MS employing a UPLC system (Vanquish, Thermo Fisher Scientific). A 2 μL aliquot of each sample was injected into a

Phenomenex Kinetex C18 (2.1 mm × 50 mm, 2.6 μm), with the sample tray kept at 4 °C. The quality control (QC) sample was prepared by mixing equal aliquots of supernatants from all samples.

The Orbitrap Exploris 120 mass spectrometer was employed due to its information-dependent acquisition (IDA) mode, controlled by the acquisition software Xcalibur (Thermo). In this mode, the acquisition software continuously assessed the full scan MS spectrum. The electrospray ionization (ESI) source conditions were configured as follows: sheath gas flow rate of 50 Arb, auxiliary gas flow rate of 15 Arb, capillary temperature of 320 °C, full MS resolution of 60,000, MS/MS resolution of 15,000, collision energy set at 10/30/60 in NCE mode, and spray voltage of 3.8 kV (positive) or 3.4 kV (negative). Metabolite annotation was performed using an in-house MS2 database (BiotreeDB).

2.6. Detection of volatile compounds

Volatile compounds were measured by headspace solid-phase microextraction coupled with gas chromatography–mass spectrometry (HS-SPME-GC–MS/MS) following the methods described by Zhang et al. (2021). One gram of moromi and 10 μL of 0.0078 g/100 mL methyl octanoate (internal standard) were ferred into a 20 mL vial with a polytetrafluoroethylene/aluminum cap. The vial was immersed in a 60 °C ± 2 °C bath for 15 min equilibration, then a 50/30 μm DVB/CAR/PDMS fiber (Supelco, Inc., Bellefonte, PA, USA) was inserted for 45 min. The volatile compounds adsorbed onto the fiber were analyzed using a GC–MS/MS system (Thermo trace 1300 gas chromatography coupled with system TSQ 9000 mass spectrometer, Thermo Electron Corporation, Waltham, MA, USA), outfitted with a VF-WAX-MS capillary column (30.0 m × 0.25 mm, 0.25 μm, Agilent, Santa Clara, USA). Volatiles were thermally desorbed in the GC injection port at 270 °C. High purity helium was utilized as carrier gas at 1 mL/min. The initial column temperature was set at 40 °C and increased to 100 °C at 4 °C/min, 230 °C at 6 °C/min, and held at 230 °C for 10 min. The GC–MS chromatograms of volatiles were acquired using EI ionization source at a fragment voltage of 70 eV, and peak identification was performed by searching the NIST2017 library, with a similarity index (SI) threshold of >800. The concentrations of volatile compounds were calculated using the following equation: $C\ (\mu g/kg) = \frac{A_1}{A_0} \times \frac{C_0 V_0}{m_1}$.where C is the concentration (μg/kg) of a volatile compound, C_0 is the concentration of the internal standard compound, A_1 is the peak area of a volatile compound, A_0 is the peak area of the internal standard compound, V_0 is a volume (μL) of the internal standard compound, and m_1 is the weight (g) of moromi.

2.7. Detection of microbial community

2.7.1. Direct counting method

Bacterial and yeast counts in moromi were determined using a hematocrit plate (Qiujing, Shanghai, China) under a microscope, with samples diluted in sterile water, vortexed for 5 min, and observed (Lan et al., 2019).

2.7.2. High-throughput sequencing

The microbial community composition in a sample during the various stages of the process was determined following the outlined method (Zhang et al., 2021). Total genomic DNA was extracted using the Fast DNA SPIN extraction kit (MP Biomedicals, Santa Ana, CA, USA) according to the manufacturer's instructions. The DNA quality and quantity were assessed by 0.8% (*w/v*) agarose gel electrophoresis and NanoDrop ND-1000 spectrophotometer (Thermo Scientific, Waltham, MA, USA), respectively. The universal primer pairs 338F/806R and ITS5/ITS1 were utilized to amplify the V3-V4 regions of bacterial 16S rRNA genes and the ITS1 region of fungal DNA, respectively. The subsequent PCR amplification and reaction systems were described in our previous study (Zhang et al., 2021). The amplicons were pooled to equal concentrations and subjected to paired-end 2 × 300-bp sequencing on the Illumina MiSeq platform with MiSeq Reagent Kit v3 (Shanghai Personal Biotechnology Co., Ltd., Shanghai, China). High-quality sequences were clustered into operational taxonomic units at 97% sequence identity using UCLUST after chimera detection.

Alpha and beta diversity indices were employed to assess species diversity within and between habitats, respectively. Chao1/Observed species and Shannon/Simpson indices were used to evaluate alpha diversity, reflecting species richness and diversity, respectively. Beta diversity was quantified by differences in distances between samples through principal coordinates analysis which is more suitable for complex structures.

2.7.3. Pipeline of metagenomics

Metagenome DNA extraction and shotgun sequencing: microbial genomic DNA was extracted using the Mag-Bind Soil DNA Kit (M5635–02) (Omega Bio-Tek, Norcross, GA, USA) according to the manufacturer's protocol. DNA concentration was measured utilizing a NanoDrop ND-1000 spectrophotometer (Thermo Fisher Scientific, Waltham, MA, USA), and its quality was assessed via 1.20% agarose gel electrophoresis. The extracted DNA underwent library preparation for metagenome shotgun sequencing, with insert sizes of 400 bp, using the Illumina TruSeq Nano DNA LT Library Preparation Kit. Subsequently, each library was sequenced using the Illumina HiSeq X-ten platform (Illumina, USA) with a PE150 strategy at Personal Biotechnology Co., Ltd. (Shanghai, China).

Sequence analysis: raw sequencing reads underwent preprocessing to obtain quality-filtered reads for subsequent analysis. Initially, sequencing adapters were removed using Cutadapt (v1.2.1), followed by trimming low-quality reads using a sliding-window algorithm. Next, reads were aligned to the host genome using BWA (Li & Durbin, 2009) to eliminate host contamination. Quality-filtered reads were then de novo assembled using IDBA-UD (Peng et al., 2012) to construct the metagenome for each sample. Subsequently, coding regions (CDS) of metagenomic scaffolds longer than 300 bp were predicted using MetaGeneMark (Zhu et al., 2010). CDS sequences from all samples were clustered at 90% protein sequence identity using CD-HIT (Fu et al., 2012) to generate a non-redundant gene catalog. Gene abundance in each sample was estimated using soap.coverage (http://soap.genomics.org.cn/) based on the number of aligned reads. Taxonomy assignment of non-redundant genes was performed by aligning them against the NCBI-NT database using BLASTN (e value <0.001).

2.7.4. Detection of the abundance of major microorganisms by quantitative real-time PCR (RT-qPCR)

The number of major microorganisms in moromi at the end was measured by RT-qPCR using an MA-6000 Real-Time PCR System (Suzhou Molarray Co., Ltd., Suzhou City, Jiangsu Province, China). Table S1 listed the primers used for RT-qPCR. The reaction mixtures (20 μL) consisted of 2 μL template DNA, 10 μL 2 × SYBR real-time PCR premixture, 0.4 μL forward primer (10 μM), and 0.4 μL reverse primer (10 μM), 7.2 μL distilled water. The amplification conditions were 95 °C for 5 min, 40 cycles at 95 °C for 15 s, and 60 °C for 30 s. The actual biomass of moromi using the absolute quantification method by calculating the number of gene copies by comparing the Cq value of the sample with a standard curve (Walker, 2001).

2.8. Statistics analysis

The analyses were performed in triplicate unless otherwise stated. Data underwent one-way analysis of variance (ANOVA) followed by Duncan's multiple range test for mean comparison using the Statistical Package for Social Sciences (SPSS for Windows: SPSS Inc., Chicago, IL, USA). Statistical significance was determined at $p < 0.05$. Principal component analysis (PCA), principal coordinate analysis (PCoA), and partial least squares discriminant analysis (PLS-DA) were conducted to visually represent the differentiation among samples utilizing SIMCA

14.1. Spearman correlation analysis was carried out using the Hmisc package within R software (v 4.1.1) to assess the correlations between abundant microbiota and selected metabolites. The network diagram was visualized using Gephi (v 0.10.1). Redundancy analysis (RDA) was conducted to unveil the associations between microbiota and key components using Canoco 5.0 software. Other data analysis and visualization were performed using R 4.1.1 with various packages including vegan, ggplot2, pheatmap, etc., alongside Origin 9.0.

3. Results and discussion

3.1. The influence of salt content on physicochemical parameters

The physicochemical parameters of moromi fermentation were analyzed (Fig. 1). Salt content significantly affected the TA contents. By day 10, LS sample led to significantly higher TA compared to MS and HS samples. In the end, the TA contents for LS, MS, and HS were 2.61 g/100 g, 2.41 g/100 g, and 2.13 g/100 g, respectively. This was consistent with the higher relative abundance (RA) of *Tetragenococcus halophilus* in the LS (Fig. 6B). Initially, the RS content increased sharply in all samples. It then declined rapidly in LS and MS, starting on days 15 and 40, respectively. In contrast, HS's RS content, after an initial gradual increase, commenced a slow decline starting on day 70. The findings showed that salt reduction enhanced microbial metabolism in the moromi, accelerating substrate depletion (Liu et al., 2023).

In the initial phase, salt had a slight effect on ethanol content. By the mid-phase, LS exceeded MS and HS, however, MS later surpassed LS, with LS still ahead of HS. This was mainly related to the dynamic proliferation of *Zygosaccharomyces rouxii* (Fig. 6C). TN and AAN trends in all samples showed an initial increase, followed by a steady rise, in the order of LS, MS, to HS. Initially, AN increased similarly across LS, MS, and HS. After ten days, MS and HS stabilized, whereas LS climbed significantly, surpassing the others. Ultimately, the TN, AAN, and AN contents for LS, MS, and HS were recorded at 2.13 g/100 g, 1.62 g/100 g, and 0.36 g/100 g; 2.03 g/100 g, 1.35 g/100 g, and 0.22 g/100 g; and 1.76 g/100 g, 1.11 g/100 g, and 0.20 g/100 g, respectively. This pattern indicated that the low salt concentrations reduced the inhibitory effects on proteases and others, as supported by Su et al. (2005).

3.2. The influence of salt content on non-volatile compounds

LC-MS/MS analysis revealed non-targeted metabolites in three moromi samples post-fermentation. The analysis identified 8534 and 9917 metabolic ion peaks in ESI+ and ESI- modes, respectively, with quality control samples stable instrument performance (Fig. 2A). In total, 2035 reliable metabolites (ESI+: 1153; ESI-: 882) were identified obtained through MS/MS search, comprising 468 organoheterocyclic compounds, 310 lipids and lipid-like molecules, 265 organic acids and derivatives, 93 fatty acids, 88 alkaloids and 61 amino acids and peptides (Fig. 2C). Notably, fatty acids like linoleic acid, pinolenic acid, palmitic acid, and oleic acid, alongside amino acids like phenylalanine and *N*-acetyl phenylalanine, and lipids such as 4 - (dimethyl amino) butanoate and glutaryl carnitine, were prominent. Non-volatile metabolite contents were significantly higher in LS and MS than in HS, with LS showing elevated levels of organic acids, benzenoids, organoheterocyclic compounds, and alkaloids, whereas HS had higher fatty acid content. The content of small peptides in MS was comparable to HS, both exceeding LS (Fig. S1B).

The development of a supervised PLS-DA model highlighted distinct separation among the three fermented moromi samples in both modes, demonstrating the model's exceptional reliability and predictive accuracy (Fig. 2B) (Wu et al., 2024). This capability facilitated the identification of discriminative metabolites between groups. Following this, a total of 1520 differential metabolites were identified based on the variables important in projection (VIP $>$ 1.0) and statistical analysis (ANOVA $p < 0.05$). Unsupervised k-means analysis exposed varying patterns of change among these differential metabolites (ANOVA $p < 0.05$) (Fig. S1A). These differential metabolites were primarily categorized into amino acids and peptides, organic acids and derivatives, lipids and lipid-like molecules, carbohydrates, organoheterocyclic

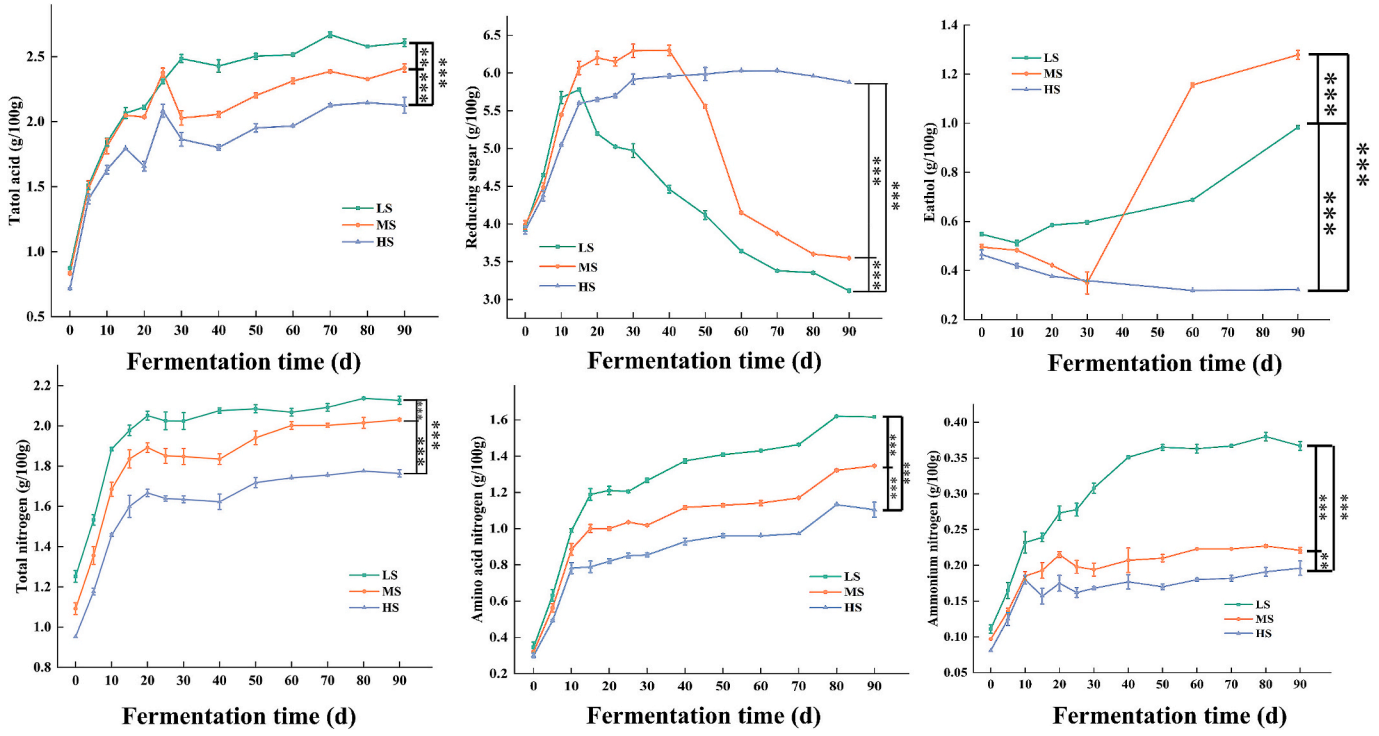

Fig. 1. Dynamic changes in physicochemical parameters of moromi during soy sauce fermentation. Soy sauce fermented with 16%, 13%, and 10% salt for HS, MS, and LS, respectively. *, $p < 0.05$; **, $p < 0.01$; ***, $p < 0.001$.

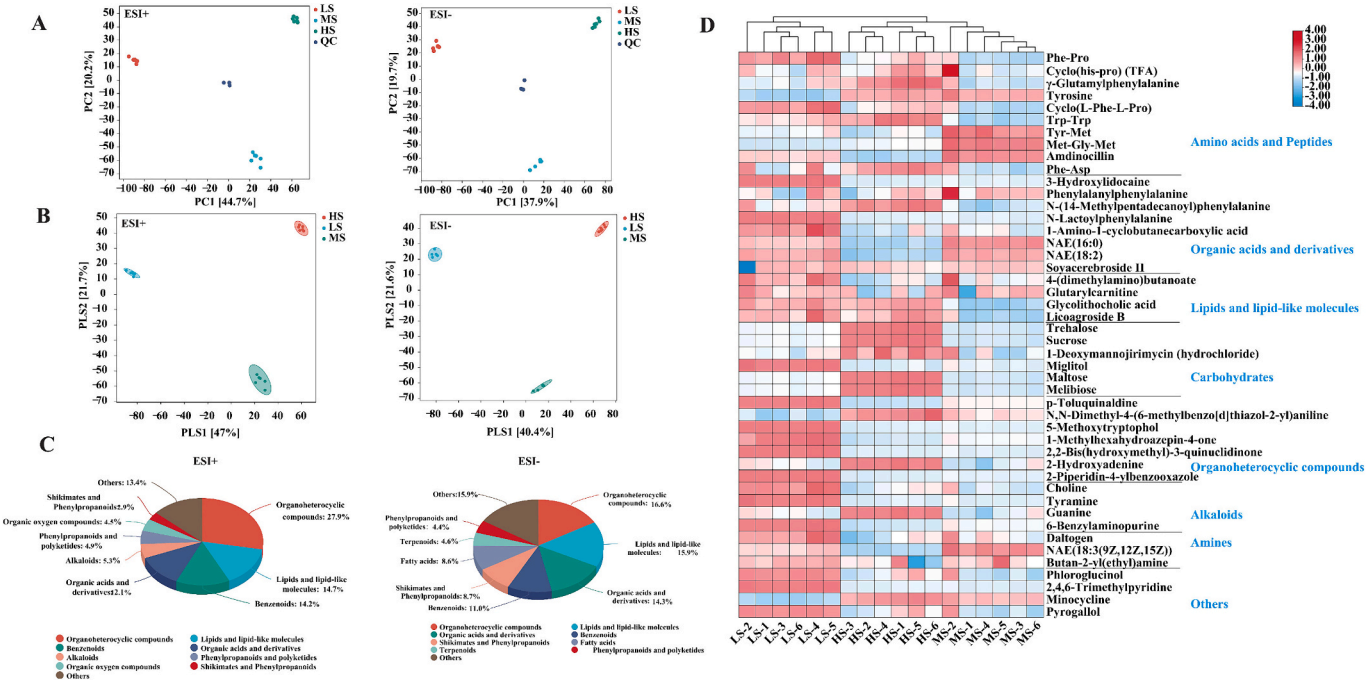

Fig. 2. Non-volatile metabolite distribution and differential metabolite screening among the three types of moromi. (A) PCA scores of positive and negative ion patterns based on metabolite characteristics. (B) Partial least squares discriminant analysis based on reliable metabolites in positive and negative ion models. (C) SUPER CLASS categorization of the three types of moromi non-volatile metabolites. (D) Cluster analysis of differential metabolites between three samples.

compounds, and alkaloids. A clustering heatmap displayed the main differential metabolites (Fig. 2D),

with bioactive peptides like Trp-Trp, Tyr-Met, Met-Gly-Met, and γ-glutamyl phenylalanine more prevalent in MS and HS than in LS, which had elevated levels of organic acids and derivatives, organoheterocyclic compounds, alkaloids, and amines.

Increased carbohydrates in HS, such as sucrose and trehalose, likely correspond to its lower microbial abundance (Fig. S1A).

Subsequent quantification of seven OAs was conducted using HPLC (Fig. 3). Oxalic acid, malic acid, and glutamic acid rose in three moromi samples, while succinic acid, citric acid, lactic acid, and acetic acid exhibited significant variations. In MS and HS, contents of succinic acid and citric acid initially rose before stabilizing, while lactic acid increased marginally. Conversely, in LS after 10 days, succinic acid and citric acid declined, while lactic acid surged to 1.56 g/100 g, significantly higher than MS and HS. The surge in lactic acid of LS samples was consistent with the rapid proliferation of *T. halophilus* and the swift proliferation of TA. This suggests that excessive salt reduction rapidly acidifies the moromi microenvironment, thereby favoring the swift growth of pathogens (Hu et al., 2023). Initially, succinic acid dominated the OA profile in all moromis (75.91%), accompanied by malic (9.05%) and citric acids (8.49%). After fermentation, MS and HS showed a prevalence of succinic (59.56%), malic (25.27%), and citric acids (7.37%), contrasting with LS where lactic and malic acids rose, while others diminished. Ultimately, the total OA content of LS, MS, and HS varied from 5.06 g/100 g, 9.22 g/100 g, and 7.76 g/100 g, respectively.

Fermentation generally increased FAAs in all samples, with the umami-flavored Glu being the most abundant (Table S2). After 10 days,

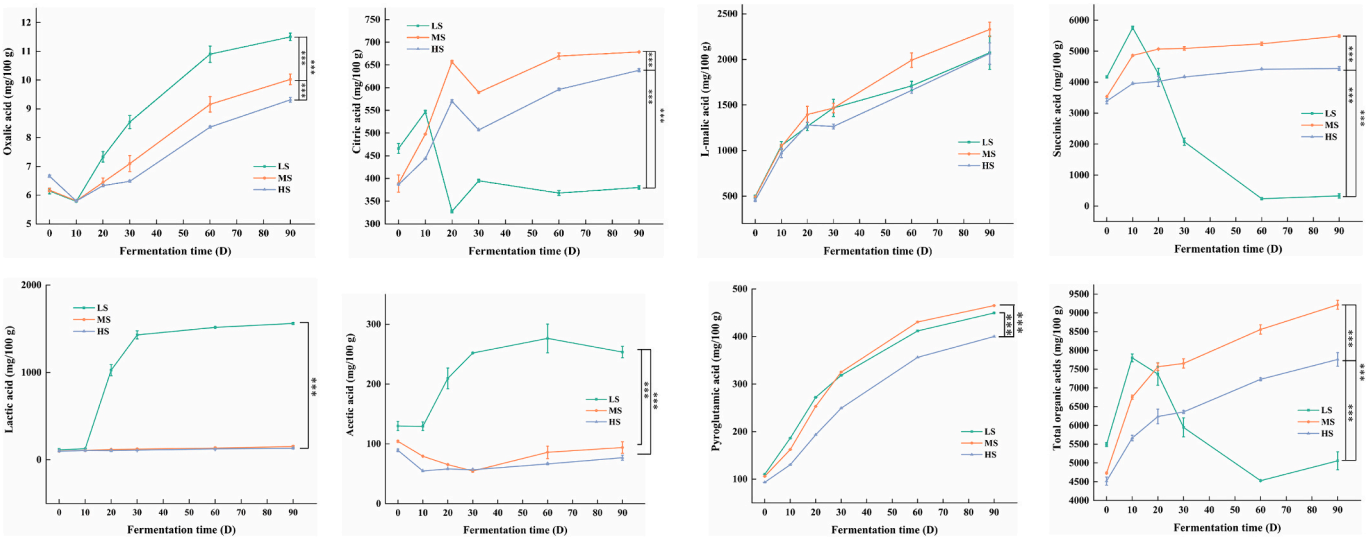

Fig. 3. Dynamic changes in organic acids of moromi during soy sauce fermentation.

FAA content in LS and MS significantly exceeded those in HS. By day 90, LS and MS were approximately 1.29 times higher. However, Asp content in LS was notably lower than in HS and MS, with Tyr and His nearly undetectable, affecting the FAAs' flavor balance, whereas MS resembled HS. These findings suggest that moderate salt reduction during fermentation enhances the content of FFA content and the synthesis of flavor compounds, including aldehydes, ketones, and pyrazines (Zhu et al., 2022).

Post-fermentation, the total BA content in LS was 4115.11 mg/kg, significantly higher than in MS (176.76 mg/kg) and HS (203.75 mg/kg) (Fig. 4). These findings indicated excessive salt reduction posed biosafety concerns (Hu et al., 2023; Liu et al., 2023; Yang et al., 2021).

3.3. The influence of salt content on volatile compounds

In this study, we identified 96 volatiles across all samples (Table S3). These included esters (37), alcohols (15), phenols (8), aldehydes (11), ketones (9), acids (3), and others (13). Notably, LS and MS showed 1.42 and 2.92 times higher volatile content than HS, respectively, indicating that reduced salt content enhanced microbial activity and volatile contents (Liu et al., 2023). Esters, alcohols, and phenols were dominant. Changes in these components spanned two phases (Fig. 5A), with esters initially making up over 80% of the volatiles. Post-fermentation, the ratio of esters to alcohols to phenols in MS and HS stabilized at 4:2:3, while LS showed a higher ester-to-alcohol ratio and lower phenol content.

The PCA model, explaining 75.38% of the variance, effectively distinguished differences among samples, highlighting key transitions at days 0 and 30 (Fig. 5B). By day 30, moromi diverged, and by the end, LS90 and MS90 were notably distinct from HS90, with significant internal variations, reflecting salt's substantial effect on soy sauce flavor (Liu et al., 2023). Cluster heatmap analysis further highlighted the unique feature of MS moromi (Fig. 5C). During fermentation, there was a reduction of four long-chain fatty acid methyl esters, such as methyl 16-methylheptadecanoate, and an increase in eight medium and long-chain fatty acid ethyl esters, for instance, ethyl acetate. This was in line with the enhanced ethanol fermentation observed in MS samples (Fig. 1). The reduction in salt content notably augmented the fatty acid esters content in the moromi, with MS exhibiting the highest content. MS also showed higher alcohol contents, particularly 1-octen-3-ol (mushroom aroma) and phenylethyl alcohol (floral and fruity aroma) (Gao et al., 2022), and total phenols and ketones were 3.84 and 4.07 times those in HS, respectively (Table S3). Notably, key components 4-EG (sauce flavor) and HEMF (caramel aroma) were 3.97 and 8.27 times higher, respectively (Gao et al., 2022). LS samples exhibited a decrease in characteristic flavors like 4-EG, 1-octen-3-ol, and benzeneacetaldehyde (honey aroma), with 4-VG (sauce flavor) even falling below detectable levels, and an uptick in undesirable flavors such as acetaldehyde and 2-methyl-1-propanol. This was consistent with the trend observed in the LS samples, where the RA of functional microorganisms such as *Weissella*, *Staphylococcus*, and *Zygosaccharomyces* decreased, while the RA of the foodborne pathogen *Ligilactobacillus pobuzihii* had significantly increased (Fig. 6 BCE). Similar patterns were also observed in reduced-salt doubanjiang and soy sauce (Hu et al., 2023; Liu et al., 2023; Yang et al., 2021).

3.4. The influence of salt content on microbial community

A hemocytometer was used to count bacteria and yeast numbers in soy sauce samples during fermentation (Fig. 6A). Bacterial counts in LS and MS surged until day 15 of fermentation and then stabilized. On day 10, LS bacterial counts were significantly higher than those in MS and HS. Ultimately, LS reached 1.47×10^9 CFU/g, which was 3.6 and 3.3 times that of MS and HS, respectively. Yeast counts in all samples were significantly lower than bacterial counts, exhibiting a fluctuating growth pattern, with no significant differences in totals by the end of the process. The results showed that a 10% salt concentration in the moromi significantly diminished the inhibitory effect on bacteria (Hu et al., 2024).

Amplicon sequencing revealed the impact of salt reduction on microbial community composition. As shown in Fig. S2A, LS samples had a lower bacterial richness, indicated by a reduced Chao1 index versus HS, but showed increased microbial evenness, with a higher Shannon index than HS and MS. The fungal community structures were similar across all samples by the end of the process.

PCoA based on Bray-Curtis distance highlighted shifts in bacterial community β-diversity in LS during the process, whereas MS and HS clustered closely together (Fig. S2B). This observation was supported by

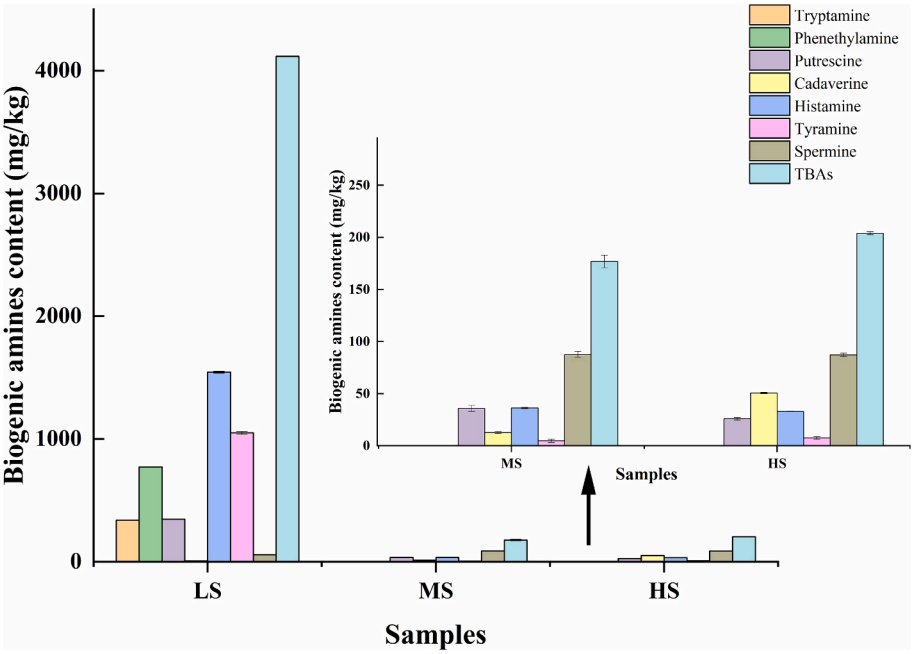

Fig. 4. The contents of biogenic amines in moromi at the end of fermentation.

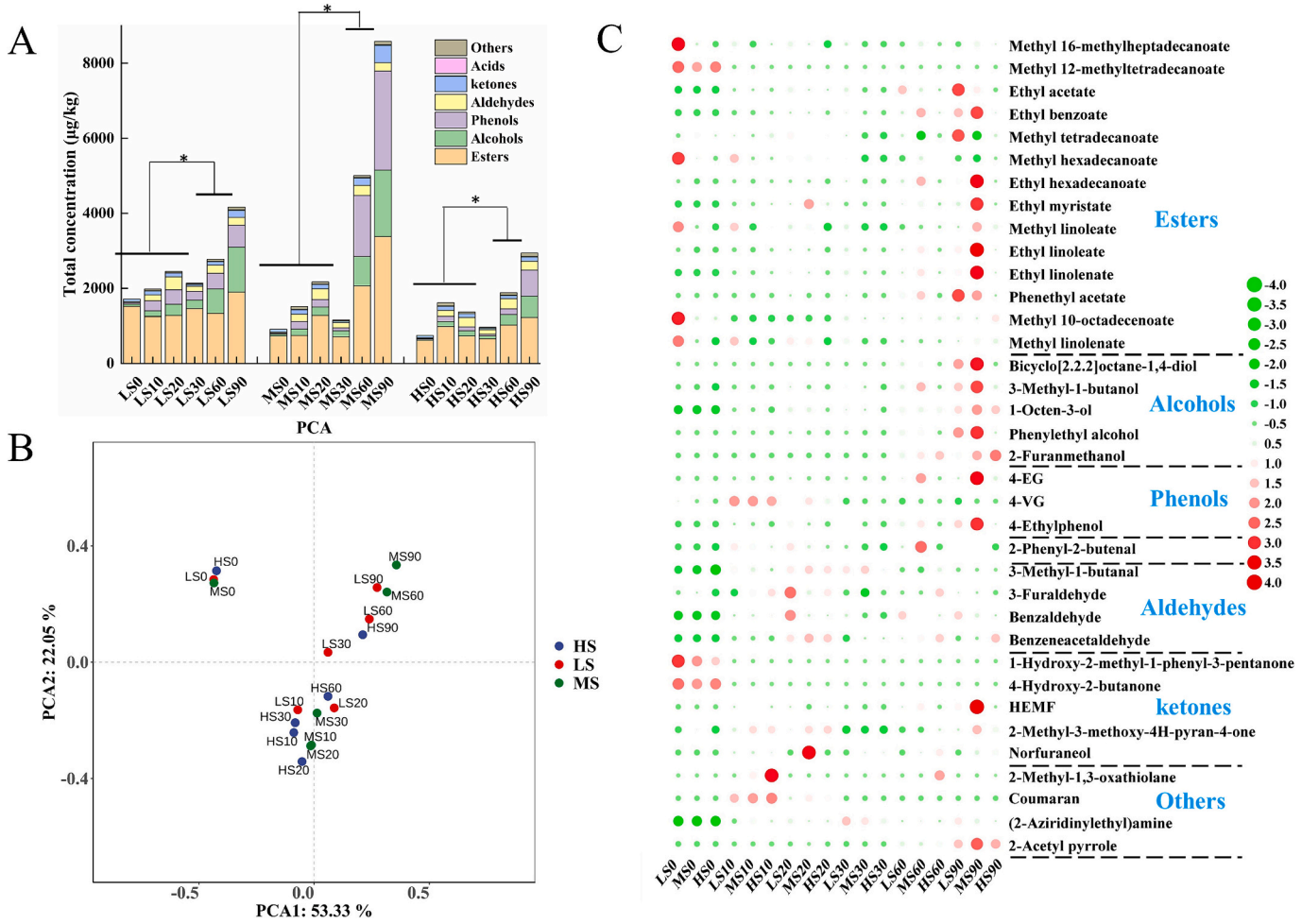

Fig. 5. Dynamic changes in volatile compounds among the three types of moromi. (A) Concentrations of volatile compounds. (B) Volatile component profiles using PCA based on Hellinger. (C) Heatmap visualization of main volatile compounds (relative content >1%) detected in these moromi.

ANOSIM analysis ($R = 0.438$, $p = 0.001$) indicating distinct microbiota dynamics in LS. For the 30th day, the fungal β-diversity among the samples showed a unified clustering, with LS and HS positioned in the first quadrant and MS in the fourth quadrant from this point onward.

The Venn diagram based on the ASV (Fig. S3) revealed differences in microbiota compositions among the three moromi samples. LS, MS, and HS harbored 207, 143, and 329 distinct bacterial genera, respectively, with 188 shared across all. LS shared 16 genera with MS, 21 with HS, and MS shared 66 genera with HS. Additionally, LS, MS, and HS contained 83, 64, and 103 unique fungal genera, respectively, with 14 genera common to all. LS shared 12 genera with MS, 6 with HS, and MS shared 6 genera with HS. The results highlighted the alterations in the microbiota composition, particularly in LS due to salt reduction.

Bacterial classification identified 14 phyla, with Firmicutes constituting over 99.00% RA in both LS and MS fermentation. However, in HS, Proteobacteria peaked at about 3.00% RA on days 20 and 30 (Fig. 6B). The fungal microbiota spanned 6 phyla, with Ascomycota dominating over 99.80% RA in all samples (Fig. 6C). Of 157 identified bacterial genera, the top 10, accounting for 95.00% of the total abundance (Fig. 6B). The fungal microbiota, comprising 82 genera, was dominated by the top 10 RA genera, which accounted for over 99.50% of the total abundance. (Fig. 6C). Initially, *Staphylococcus* (RA > 83.00%) and *Weissella* (RA > 8.00%) were dominant in all moromi samples (Fig. 6B). By day 10, increases in RA of *Ligilactobacillus* and *Tetragenococcus* led to distinct microbiota structures. By day 20, *Tetragenococcus* in LS dominated with an RA over 75%, possibly due to the weaker acid tolerance of *Staphylococcus* and *Weissella*, whose RA plummeted to levels occasionally undetectable (Zhang et al., 2021). Similar trends were observed in low-salt soy sauce and doubanjiang (Hu et al., 2023; Yang et al., 2021). In MS and HS, *Staphylococcus* dominated with an RA > 80.00%, while *Weissella* RA varied from 8.11 to 12.49% in MS and 3.89–15.53% in HS. *Luteimonas* was detected only in HS, with salinophilicity, and some strains' cellulose and denitrification capacity (Zhou et al., 2021).

Aspergillus RA in three moromi samples exceeded 88.25% before day 30 of fermentation (Fig. 6C). *Zygosaccharomyces* was unique to LS, with an RA ranging from 0 to 10.88%. After 30 days, significant changes were noted in the fungal community structure (Jiang, Chen, et al., 2023). *Starmerella* and *Wickerhamiella* dominated, together comprising over 96.34% RA. In MS, *Starmerella* and *Zygosaccharomyces* RA rose to 54.56% and 35.65%, respectively, whereas *Wickerhamiella* RA decreased, indicating that high ethanol content resulted from shifts in fungal community structure. In HS, *Wickerhamiella* and *Aspergillus* were predominant, with RAs exceeding 71.84% and 20.00%, respectively.

To validate the amplicon sequencing results' objectivity, shotgun metagenomics analyzed the microbiota structure in post-fermentation moromi for differences. The proportion of effective sequences and base numbers exceeded 97.00% for all samples, indicating the reliability of the sequencing data. Species profiles differed among samples (Fig. 6D). *T. halophilus* RA in LS, MS, and HS was 55.90%, 1.69%, and 1.30%, respectively. *L. pobuzihii* had an RA of 18.53% in LS, versus 0.04% in MS and 0.02% in HS. Functional bacteria, such as *Staphylococcus*, *Mammaliicoccus*, and *Weissella*, dominated in MS (Feng et al., 2023; Zhang et al., 2021). *Staphylococcus gallinarum*, *Staphylococcus*

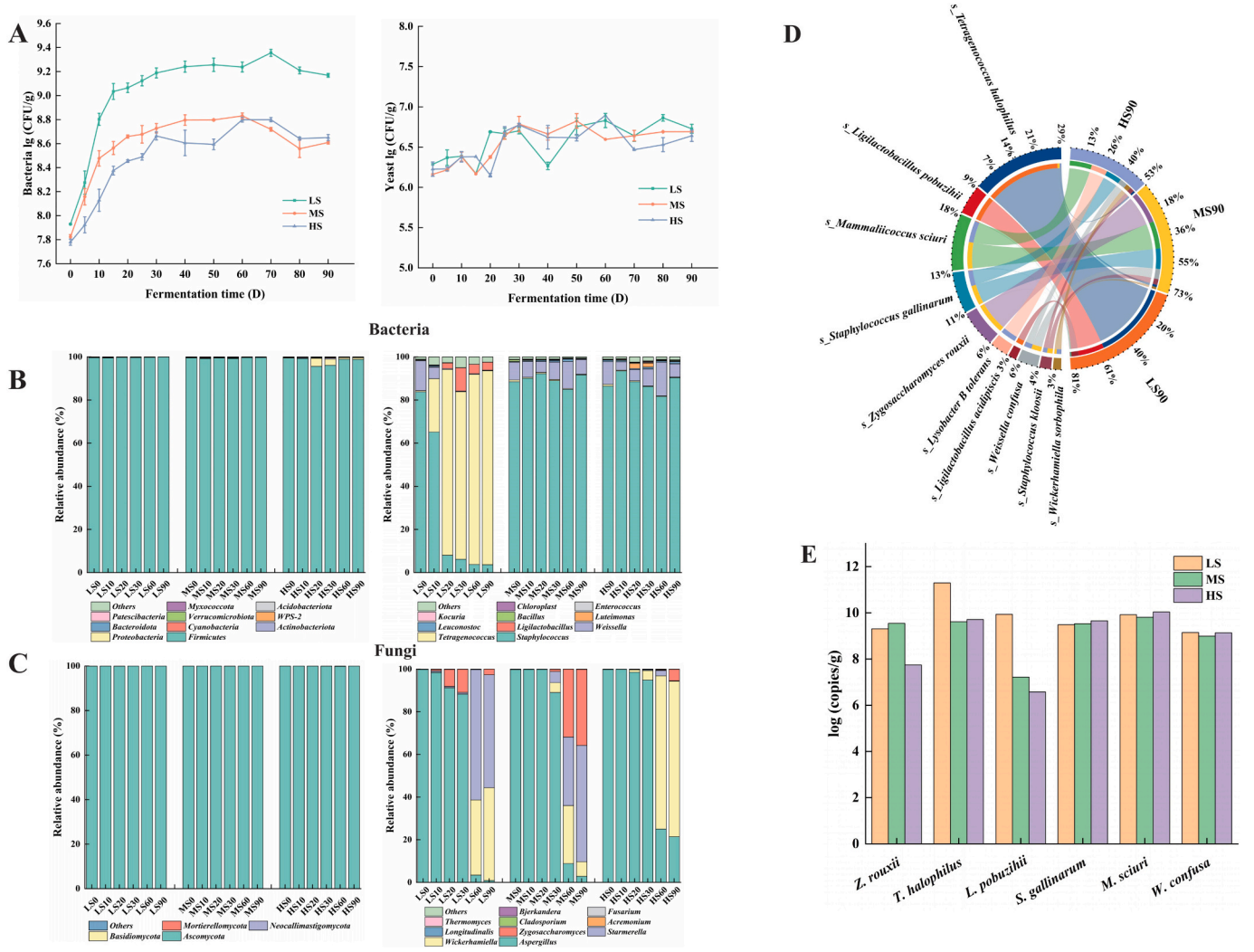

Fig. 6. Analysis of the dynamics of microbial community during soy sauce fermentation. (A) Changes of biomass of total bacteria and yeasts. (B) Relative abundance of bacterial phylum and genera. (C) Relative abundance of fungal phylum and genera. (D) Relative abundance of bacterial and fungal species. (E) Comparison of the populations of differential microorganisms in moromi.

kloosii, *Mammaliicoccus sciuris* and *Weissella confusa* exhibited RA of 15.35%, 4.02%, 19.79%, and 7.44%, respectively. Functional fungi *Z. rouxii* and *Wickerhamiella sorbophila* RA in MS were 23.24% and 1.61%, respectively (Wang et al., 2024). The bacterial community structure in HS was similar to that in MS, with RAs of *M. sciuri*, *S. gallinarum*, *Lysobacter tolerans*, *W. confusa,* and *S. kloosii* of 15.89%, 11.81%, 11.56%, 5.65%, and 3.08%, respectively. *L. tolerans*, reported to be symbiotic with plants (Brescia et al., 2020), was detected only in HS. In HS, *W. sorbophila* RA was 3.49%, compared to *Z. rouxii* at 0.10%.

Absolute quantification of the major bacterial and fungal species was performed based on the copy numbers of 16S rRNA and ITS genes (Fig. 6E). In LS, *T. halophilus* and L. *pobuzihii* had copy numbers of 1.96 $\times$ 10^{12} copies/g and 8.60 $\times$ 10^{9} copies/g, respectively, which were significantly higher than those in MS and HS. In MS, the copy number of *Z. rouxii* was 3.49 $\times$ 10^{9} copies/g, substantially higher than in LS and HS. High salt affected the survival of *Z. rouxii* in later stages, while low salt levels favored the overgrowth of *T. halophilus* and L. *pobuzihii*.

3.5. The influence of salt content on community interactions

Co-occurrence network analysis showed salinity significantly affected community interactions (Fig. 7). The LS network exhibited 794 edges, with an average degree and clustering coefficient of 15.88 and 0.89, respectively (Fig. 7A), surpassing those of MS and HS. This indicated that a substantial reduction in salinity diminished microbial suppression, leading to a more complex network structure. In the microbial network, highly associated species were grouped into modules, where interactions between species were stronger and more frequent highlighting a more intricate community structure (Ling et al., 2022). Networks in MS and HS conditions had a greater number of modules and higher modularity compared to LS, suggesting specialized species interactions under these conditions. In MS and HS, the proportions of negatively correlated connections were 5.42% and 5.02%, respectively, which were higher than the 3.02% observed in LS, contributing to increased network robustness (Yuan et al., 2021).

The top 20 RA bacteria and fungi genera, with >20% coverage in each group, showed main microbial interactions among them (Fig. 7B). In LS, bacterial genera primarily interacted, with a lower involvement of fungi. These bacterial genera included *Tetragenococcus*, *Streptococcus*, *Staphylococcus*, *Weissella*, *Bacillus*, *Kocuria*, and *Enterococcus*, with the latter two being less dominant in the soy sauce fermentation processes (Feng et al., 2023). *Tetragenococcus*, which had the highest RA in LS, was negatively correlated with *Weissella*, *Staphylococcus*, *Streptococcus,* and *Bacillus*, possibly due to its rapid proliferation at low salinity, leading to over-acidification and disruption of the microbiota balance (Gao, Zhao, et al., 2023). Conversely, in MS, *Tetragenococcus* was positively

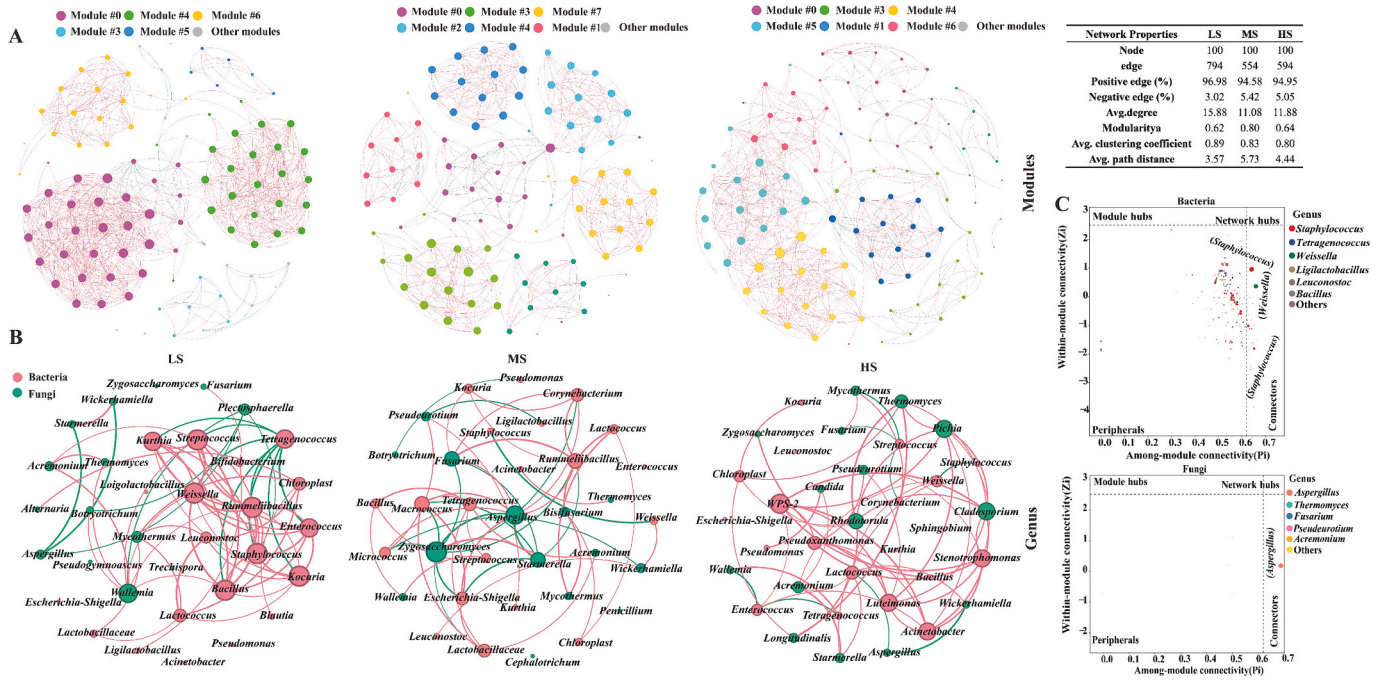

Fig. 7. Co-occurrence network of ASVs from soy sauce samples. Each node represents an ASV. An edge represents the correlation between ASVs. Red lines indicate positive correlations and green lines for negative correlations. The area of the node is proportional to node degree, calculated from correlations of abundances for each ASV. These coefficients were statistically significant ($P < 0.05$, $|\rho| > 0.6$). (A) Network of moromi microbial populations based on modular. (B) Relationships among major microbial genera. The relative abundance of bacteria and fungi in the top 20, and microbial genera with at least 20% coverage in each group. (C) Screening of key microorganisms by zi-pi figure. (For interpretation of the references to colour in this figure legend, the reader is referred to the web version of this article.)

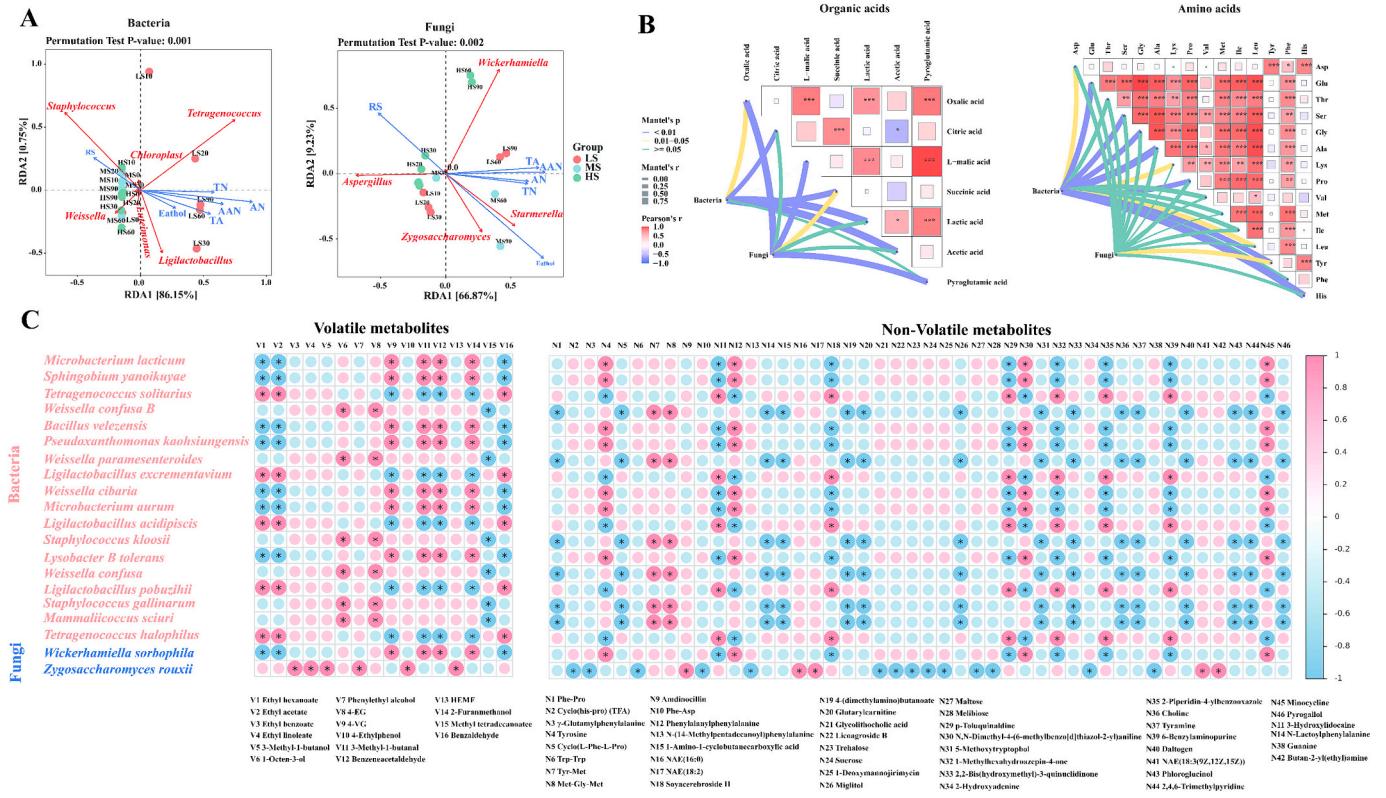

Fig. 8. Correlations between differential microbes and main metabolites. (A) Correlations of major genera with physicochemical parameters were constructed by redundancy analysis (RDA). (B) Correlations of major genera with organic acids and free amino acids were constructed by mantel analysis. (C) Correlations of major species with major volatile and non-volatile metabolites were constructed by clustering heat map. * $p < 0.05$; **, $p < 0.01$; ***, $p < 0.001$.

correlated with *Streptococcus*, *Bacillus*, and *Lactobacillaceae*, enhancing their growth and improving interactions with *Zygosaccharomyces*, *Starmerella,* and *Aspergillus*. For instance, *Zygosaccharomyces* was correlated positively with *Starmerella* but negatively with bacteria such as *Corynebacterium*, *Macrococcus,* and *Micrococcus*. MS increased the RA of *Zygosaccharomyces* (Fig. 6C,D) and promoted alcoholic fermentation (Fig. 1). The synergistic effects of ethanol and salinity further inhibited foodborne pathogens. In HS, similar to MS, both bacterial and fungal microbiota showed higher co-occurrence, altering genus interrelations. For example, strong correlations were observed among bacterial genera such as *Luteimonas*, *Acinetobacter*, *WPS-2*, *Streptococcus*, *Weissella*, *Staphylococcus*, and *Bacillus*, as well as among fungal genera such as *Pichia*, *Thermomyces*, *Rhodotorula*, *Zygosaccharomyces*, and *Aspergillus*. This indicated that a moderate reduction in salt content (MS) improved the core module interactions of key genera in HS, addressing the microbial imbalance observed in LS.

Analyzing the within-module connectivity (Zi) and among-module connectivity (Pi), key taxa in the moromi microbiota network were identified (Fig. 7C) (Jiang, Zhang, et al., 2023). Key microbes included *Staphylococcus*, *Weissella*, and *Aspergillus*, with *Staphylococcus* and *Weissella* dominant in both HLF and Cantonese soy sauce (Feng et al., 2023; Jiang, Chen, et al., 2023), positively correlated with essential metabolites like OAs and various flavor compounds (HEMF, 3-methyl-1-butanol, ethyl hexanoate, ethyl acetate, *etc*). *A. oryzae*, a dominant fungus in koji, influenced nutritional networks via enzymes like amylase, protease, and cellulase, significantly affecting interspecific moromi microbiota interactions (Zhong et al., 2018). Thus, these key microbes were crucial for community assembly, stability, and metabolic functions (Banerjee et al., 2018).

3.6. Correlation of microbial communities with metabolites

RDA highlighted the correlation between physicochemical properties and microbial communities (Fig. 8A). The total explained variance and the global permutation test *p*-value of the bacterial model were 86.90% and 0.001, respectively, surpassing those of the fungal model at 76.10% and 0.002. This indicated a more pronounced impact of physicochemical properties on the changes in the bacterial community structure, aligning with Fig. 6A. Within the bacterial community, LS separated distinctly on the RDA1 axis, correlating *Tetragenococcus* and *Ligilactobacillus* with TA, AN, and AAN. The association elucidated the over-acidification of the microenvironment and the rapid substrate hydrolysis observed in LS samples (Xiang et al., 2022). Conversely, in MS and HS bacterial communities, a positive correlation was observed between *Weissella* and *Staphylococcus* with RS. Notably, RS and ethanol influenced the fungal microbiota, with *Aspergillus* correlating with RS and *Zygosaccharomyces* and *Starmerella* positively correlating with ethanol in MS (Gao, Zhao, et al., 2023).

The Mantel test showed that differences in the microbiota significantly affected the contents of OAs and FAAs (Fig. 8B). Bacteria were primarily associated with the production of OAs, including citric acid, lactic acid, succinic acid, and acetic acid, whereas fungi significantly correlated with oxalic acid, malic acid, and pyroglutamic acid. Bacteria also significantly influenced FAAs, particularly Glu, Ser, Gly, Tyr, and His. These FAAs are crucial for the development of soy sauce's flavor profile (Zhu et al., 2022). This was primarily because, during soy sauce fermentation, the predominant halotolerant lactic acid bacteria(Gao, Zhao, et al., 2023), increased their metabolic activity when salt levels decreased.

A correlation heatmap linking the top 20 species to differential metabolites was constructed using metagenomics and metabolomics data (Fig. 8C). Bacteria exhibited significant positive correlations with 9 volatile and 12 non-volatile compounds, indicating their substantial contribution to the metabolic profile of soy sauce. *Staphylococcus* and *Weissella*, the principal functional microbes in Chinese soy sauce fermentation, are essential for the hydrolysis of raw materials, organic acid production, and the synthesis of flavor compounds, such as esters and phenols, which are critical for shaping the distinctive taste and aroma of the soy sauce (Feng et al., 2023; Gao, Zhao, et al., 2023). Notably, within these genera, specific species like *W. confusa*, *W. paramesenteroides*, *S. kloosii*, and *S. gallinarum* have been found to correlate positively with key flavor compounds such as 1-octen-3-ol and 4-EG (Fig. 8C), which contribute to the characteristic soy sauce aroma. Additionally, these species are associated with bioactive peptides like Tyr-Met and Met-Gly-Met, which have potential health benefits (Erdmann et al., 2006). The results confirmed their role in the complex biochemical transformations that occur during the fermentation process. *T. halophilus*, *L. excrementavium*, *L. acidipiscis*, and L. *pobuzihii* showed significant negative correlations with 4-VG, 3-methyl-1-butanal, benzeneacetaldehyde, and 2-furanmethanol, while positively correlating with 1 alkaloid, 2 OAs, and 3 heterocyclic compounds (Fig. 8C). The findings explained the diminished presence of key flavors and the emergence of off-flavors in LS samples. *Z. rouxii* and *W. sorbophila* positively correlated with 10 volatiles, 9 non-volatiles, and significantly with 6 major volatile compounds, including HEMF and phenylethyl alcohol, and also with Phe-Asp, two long-chain fatty acids (NAE(16:0), NAE(18:2)), and 5 other differential metabolites. This also elucidates why MS samples exhibited a better flavor, highlighting the crucial role of yeast metabolism in the fermentation process of reduced-salt soy sauce (Hu et al., 2024).

4. Conclusion

This study comprehensively examined how varying salt concentrations affected the fermentation process and flavor profile of soy sauce, demonstrating that changes in salt content significantly impacted the microbiota dynamics, physicochemical properties, and metabolic profile of the moromi. Salt reduction increased TA and FAA while also presenting risks in LS samples, including increased pathogen RA, BAs, and decreased key volatiles. MS samples had elevated AAN, non-volatiles, and volatiles, surpassing HS levels, while also displaying lower lactic acid and BAs than LS samples. The study also highlighted the positive role of beneficial microbes like *S. gallinarum*, *W. confusa*, and *Z. rouxii* in increasing ethanol and small peptides while inhibiting pathogens, leading to enhanced microbial interactions for balanced fermentation in MS samples. The physicochemical properties significantly impact bacterial community structure and the correlations between key microbes and flavor compounds. Further research is necessary to develop and optimize strategies that can effectively balance these aspects, enabling the production of soy sauce that is both flavorful and compliant with health guidelines.

CRediT authorship contribution statement

Lin Zhang: Writing – original draft, Software, Methodology, Data curation. **Zhu Zhang:** Investigation, Formal analysis, Data curation. **Jun Huang:** Supervision, Resources. **Rongqing Zhou:** Writing – review & editing, Supervision, Resources, Formal analysis, Conceptualization. **Chongde Wu:** Supervision, Conceptualization.

Declaration of competing interest

The authors declare that the research was conducted in the absence of any commercial or financial relationships that could be construed as a potential conflict of interest.

Data availability

Data will be made available on request.

Acknowledgments

This work was supported by the Science and Technology Department of Sichuan Province of China (No: 23JYC0056).

Appendix A. Supplementary data

Supplementary data to this article can be found online at https://doi.org/10.1016/j.fochx.2024.101722.

References

Banerjee, S., Schlaeppi, K., & van der Heijden, M. G. A. (2018). Keystone taxa as drivers of microbiome structure and functioning. *Nature Reviews Microbiology, 16*(9), Article 9. https://doi.org/10.1038/s41579-018-0024-1

Brescia, F., Pertot, I., & Puopolo, G. (2020). Chapter 16—Lysobacter. In M. Senthil Kumar, K. Annapurna, K. Kumar, & A. Sankaranarayanan (Eds.), *N. Amaresan* (pp. 313–338). Beneficial Microbes in Agro-Ecology: Elsevier. https://doi.org/10.1016/B978-0-12-823414-3.00016-2.

Chang, H., Gu, C., Wang, M., Chang, Z., Zhou, J., Yue, M., Chen, J., Qin, X., & Feng, Z. (2024). Integrating shotgun metagenomics and metabolomics to elucidate the dynamics of microbial communities and metabolites in fine flavor cocoa fermentation in Hainan. *Food Research International, 177*, Article 113849. https://doi.org/10.1016/j.foodres.2023.113849

Crowe-White, K. M., Baumler, M., Gradwell, E., Juturu, V., White, D. A., & Handu, D. (2023). Application of umami tastants for sodium reduction in food: An evidence analysis center scoping review. *Journal of the Academy of Nutrition and Dietetics, 123*(11), 1606–1620. https://doi.org/10.1016/j.jand.2022.08.002

Erdmann, K., Grosser, N., Schipporeit, K., & Schröder, H. (2006). The ACE inhibitory dipeptide met-Tyr diminishes free radical formation in human endothelial cells via induction of heme oxygenase-1 and ferritin. *The Journal of Nutrition, 136*(8), 2148–2152. https://doi.org/10.1093/jn/136.8.2148

Feng, Y., Cai, Y., Su, G., Zhao, H., Wang, C., & Zhao, M. (2014). Evaluation of aroma differences between high-salt liquid-state fermentation and low-salt solid-state fermentation soy sauces from China. *Food Chemistry, 145*, 126–134. https://doi.org/10.1016/j.foodchem.2013.07.072

Feng, Y., Xie, Z., Huang, M., Tong, X., Hou, S., Tin, H., & Zhao, M. (2023). Decoding temperature-driven microbial community changes and flavor regulation mechanism during winter fermentation of soy sauce. *Food Research International.* , Article 113756. https://doi.org/10.1016/j.foodres.2023.113756

Fu, L., Niu, B., Zhu, Z., Wu, S., & Li, W. (2012). CD-HIT: Accelerated for clustering the next-generation sequencing data. *Bioinformatics (Oxford, England), 28*(23), 3150–3152. https://doi.org/10.1093/bioinformatics/bts565

Gao, X., Li, C., He, R., Zhang, Y., Wang, B., Zhang, Z.-H., & Ho, C.-T. (2023). Research advances on biogenic amines in traditional fermented foods: Emphasis on formation mechanism, detection and control methods. *Food Chemistry, 405*, Article 134911. https://doi.org/10.1016/j.foodchem.2022.134911

Gao, X., Shan, P., Feng, T., Zhang, L., He, P., Ran, J., Fu, J., & Zhou, C. (2022). Enhancing selenium and key flavor compounds contents in soy sauce using selenium-enriched soybean. *Journal of Food Composition and Analysis, 106*, Article 104299. https://doi.org/10.1016/j.jfca.2021.104299

Gao, X., Zhao, X., Hu, F., Fu, J., Zhang, Z., Liu, Z., Wang, B., He, R., Ma, H., & Ho, C.-T. (2023). The latest advances on soy sauce research in the past decade: Emphasis on the advances in China. *Food Research International, 173*, Article 113407. https://doi.org/10.1016/j.foodres.2023.113407

Hu, G., Chen, J., Du, G., & Fang, F. (2023). Moromi mash dysbiosis trigged by salt reduction is relevant to quality and aroma changes of soy sauce. *Food Chemistry, 406*, Article 135064. https://doi.org/10.1016/j.foodchem.2022.135064

Hu, G., Wang, Y., Chen, J., Du, G., & Fang, F. (2024). Synergistic fermentation with functional bacteria for production of salt-reduced soy sauce with enhanced aroma and saltiness. *Food Bioscience, 57*, Article 103459. https://doi.org/10.1016/j.fbio.2023.103459

Jiang, M., Chen, S., Lu, X., Guo, H., Chen, S., Yin, X., Li, H., Dai, G., & Liu, L. (2023). Integrating genomics and metabolomics for the targeted discovery of new Cyclopeptides with antifungal activity from a marine-derived fungus Beauveria felina. *Journal of Agricultural and Food Chemistry, 71*(25), 9782–9795. https://doi.org/10.1021/acs.jafc.3c02415

Jiang, X., Zhang, W., Li, L., Xiao, Z., Tang, J., Wu, C., Luo, X., & Zhou, S. (2023). Characteristics of microbial community, taste, aroma of high-salt liquid-state secondary fortified fermented soy sauce. *LWT - Food Science and Technology, 182*, Article 114792. https://doi.org/10.1016/j.lwt.2023.114792

Kingwascharapong, P., Paewpisakul, P., Sripoovieng, W., Sanprasert, S., Pongsetkul, J., Meethong, R., … Rawdkuen, S. (2024). Development of fish snack (Keropok) with sodium reduction using alternative salts (KCl and $CaCl_2$). *Future Foods, 9*, Article 100285. https://doi.org/10.1016/j.fufo.2023.100285

Lan, H., Wu, L., Fan, K., Sun, R., Yang, G., Zhang, F., Yang, K., Lin, X., Chen, Y., Tian, J., & Wang, S. (2019). Set3 is required for asexual development, aflatoxin biosynthesis, and fungal virulence in *aspergillus flavus*. *Frontiers in Microbiology, 10*. https://www.frontiersin.org/journals/microbiology/articles/10.3389/fmicb.2019.00530.

Li, H., & Durbin, R. (2009). Fast and accurate short read alignment with burrows-wheeler transform. *Bioinformatics (Oxford, England), 25*(14), 1754–1760. https://doi.org/10.1093/bioinformatics/btp324

Ling, N., Wang, T., & Kuzyakov, Y. (2022). Rhizosphere bacteriome structure and functions. *Nature Communications, 13*(1), Article 1. https://doi.org/10.1038/s41467-022-28448-9

Liu, H., Yang, S., Liu, J., Lu, J., & Wu, D. (2023). Effect of salt concentration on Chinese soy sauce fermentation and characteristics. *Food Bioscience, 53*, Article 102825. https://doi.org/10.1016/j.fbio.2023.102825

Peng, Y., Leung, H. C. M., Yiu, S. M., & Chin, F. Y. L. (2012). IDBA-UD: A de novo assembler for single-cell and metagenomic sequencing data with highly uneven depth. *Bioinformatics, 28*(11), 1420–1428. https://doi.org/10.1093/bioinformatics/bts174

Penland, M., Pawtowski, A., Pioli, A., Maillard, M.-B., Debaets, S., Deutsch, S.-M., Falentin, H., Mounier, J., & Coton, M. (2022). Brine salt concentration reduction and inoculation with autochthonous consortia: Impact on protected designation of origin nyons black table olive fermentations. *Food Research International, 155*, Article 111069. https://doi.org/10.1016/j.foodres.2022.111069

Singracha, P., Niamsiri, N., Visessanguan, W., Lertsiri, S., & Assavanig, A. (2017). Application of lactic acid bacteria and yeasts as starter cultures for reduced-salt soy sauce (moromi) fermentation. *LWT - Food Science and Technology, 78*, 181–188. https://doi.org/10.1016/j.lwt.2016.12.019

Su, N.-W., Wang, M.-L., Kwok, K.-F., & Lee, M.-H. (2005). Effects of temperature and sodium chloride concentration on the activities of proteases and amylases in soy sauce koji. *Journal of Agricultural and Food Chemistry, 53*(5), 1521–1525. https://doi.org/10.1021/jf0486390

Walker, N. J. (2001). Real-time and quantitative PCR: Applications to mechanism-based toxicology. *Journal of Biochemical and Molecular Toxicology, 15*(3), 121–127. https://doi.org/10.1002/jbt.8

Wang, J., Xie, Z., Feng, Y., Huang, M., & Zhao, M. (2024). Co-culture of *Zygosaccharomyces rouxii* and *Wickerhamiella versatilis* to improve soy sauce flavor and quality. *Food Control, 155*, Article 110044. https://doi.org/10.1016/j.foodcont.2023.110044

Wang, M., Kuang, S., Wang, X., Kang, D., Mao, D., Qian, G., Cai, X., Tan, M., Liu, F., & Zhang, Y. (2021). Transport of amino acids in soy sauce desalination process by electrodialysis. *Membranes, 11*(6), Article 6. https://doi.org/10.3390/membranes11060408

Wu, J., He, T., Wang, Z., Mao, J., & Sha, R. (2024). The dynamic analysis of non-targeted metabolomics and antioxidant activity of Dendrobium officinale Kimura et Migo by the synergistic fermentation of bacteria and enzymes. *LWT - Food Science and Technology, 203*, Article 116354. https://doi.org/10.1016/j.lwt.2024.116354

Xiang, S., Liu, Y., Lu, F., Zhang, Q., Wang, Y., Xiong, J., Huang, Z., Yu, Z., Ruan, R., & Cui, X. (2022). The combination of aerobic and microaerobic promote hydrolysis and acidification of rice straw and pig manure: Balance of insoluble and soluble substrate. *Bioresource Technology, 350*, Article 126880. https://doi.org/10.1016/j.biortech.2022.126880

Yang, X., Hu, W., Xiu, Z., Jiang, A., Yang, X., Sarengaowa, Ji, Y., Guan, Y., & Feng, K. (2020). Microbial dynamics and volatilome profiles during the fermentation of Chinese northeast sauerkraut by *Leuconostoc mesenteroides* ORC 2 and *Lactobacillus plantarum* HBUAS 51041 under different salt concentrations. *Food Research International, 130*, Article 108926. https://doi.org/10.1016/j.foodres.2019.108926

Yang, Y., Niu, C., Shan, W., Zheng, F., Liu, C., Wang, J., & Li, Q. (2021). Physicochemical, flavor and microbial dynamic changes during low-salt doubanjiang (broad bean paste) fermentation. *Food Chemistry, 351*, Article 128454. https://doi.org/10.1016/j.foodchem.2020.128454

Yuan, M. M., Guo, X., Wu, L., Zhang, Y., Xiao, N., Ning, D., … Zhou, J. (2021). Climate warming enhances microbial network complexity and stability. *Nature Climate Change, 11*(4), 343–348. https://doi.org/10.1038/s41558-021-00989-9

Zhang, D., Li, H., Emara, A. M., Wang, Z., Chen, X., & He, Z. (2020). Study on the mechanism of KCl replacement of NaCl on the water retention of salted pork. *Food Chemistry, 332*, Article 127414. https://doi.org/10.1016/j.foodchem.2020.127414

Zhang, L., Huang, J., Zhou, R., Qi, Q., Yang, M., Peng, C., Wu, C., & Jin, Y. (2021). The effects of different coculture patterns with salt-tolerant yeast strains on the microbial community and metabolites of soy sauce moromi. *Food Research International, 150*, Article 110747. https://doi.org/10.1016/j.foodres.2021.110747

Zhang, L., Zhang, Z., Huang, J., Zhou, R., & Wu, C. (2024). Co-culture of *Tetragenococcus halophilus* and *Zygosaccharomyces rouxii* to improve microbiota and metabolites in secondary fortified fermented soy sauce. *Food Bioscience.* , Article 104850. https://doi.org/10.1016/j.fbio.2024.104850

Zhong, Y., Lu, X., Xing, L., Ho, S. W. A., & Kwan, H. S. (2018). Genomic and transcriptomic comparison of *aspergillus oryzae* strains: A case study in soy sauce koji fermentation. *Journal of Industrial Microbiology & Biotechnology, 45*(9), 839–853. https://doi.org/10.1007/s10295-018-2059-8

Zhou, J., Chen, J., Ma, J., Xu, N., Xin, F., Zhang, W., Zhang, H., Dong, W., & Jiang, M. (2021). *Luteimonas wenzhouensis* Sp. Nov., A Chitinolytic Bacterium Isolated from a Landfill Soil. *Current Microbiology, 78*(1), 383–388. https://doi.org/10.1007/s00284-020-02293-9

Zhu, L., He, S., Lu, Y., Gan, J., Tao, N., Wang, X., Jiang, Z., Hong, Y., & Xu, C. (2022). Metabolomics mechanism of traditional soy sauce associated with fermentation time. *Food Science and Human Wellness, 11*(2), 297–304. https://doi.org/10.1016/j.fshw.2021.11.023

Zhu, W., Lomsadze, A., & Borodovsky, M. (2010). Ab initio gene identification in metagenomic sequences. *Nucleic Acids Research, 38*(12), Article e132. https://doi.org/10.1093/nar/gkq275